

*Wariff* 1

Technical Report No. 85

SACLANT ASW  
RESEARCH CENTRE

IMPULSE RESPONSE OF A LAYERED BOTTOM

by

OLE F. HASTRUP

15 JANUARY 1967

NATO

VIALE SAN BARTOLOMEO, 400  
LA SPEZIA, ITALY

This document is released to a NATO Government at the direction of the SACLANTCEN subject to the following conditions:

1. The recipient NATO Government agrees to use its best endeavours to ensure that the information herein disclosed, whether or not it bears a security classification, is not dealt with in any manner (a) contrary to the intent of the provisions of the Charter of the Centre, or (b) prejudicial to the rights of the owner thereof to obtain patent, copyright, or other like statutory protection therefor.

2. If the technical information was originally released to the Centre by a NATO Government subject to restrictions clearly marked on this document the recipient NATO Government agrees to use its best endeavours to abide by the terms of the restrictions so imposed by the releasing Government.

UNCLASSIFIED



TECHNICAL REPORT NO. 85

SACLANT ASW RESEARCH CENTRE  
Viale San Bartolomeo 400  
La Spezia, Italy

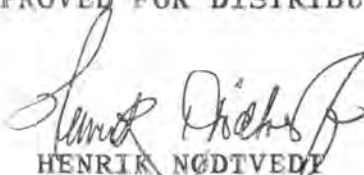
IMPULSE RESPONSE OF A LAYERED BOTTOM

By

O. Hastrup

15 January 1967

APPROVED FOR DISTRIBUTION



HENRIK NØDTVEDT

Director

UNCLASSIFIED

Manuscript Completed:

6 October 1966



## TABLE OF CONTENTS

	<u>Page</u>
ABSTRACT	1
INTRODUCTION	2
1. IMPULSE RESPONSE	3
1.1 Theory	3
1.2 Numerical Calculations	5
2. NUMERICAL EXAMPLE	11
REFERENCES	13
FIGURES	14



# IMPULSE RESPONSE OF A LAYERED BOTTOM

By

O. Hastrup

## ABSTRACT

Numerical methods are used for the Fourier inversion of the frequency-dependent loss transfer function. Because of the non-zero finite values of the integrand for an infinite high frequency, the asymptotic value is subtracted from the integral, thereby making it possible to use a finite truncation frequency in the calculation of the remainder integral. The influence of a correct asymptotic value, truncation frequency, and frequency increment is shown in graphs.

The impulse response is calculated at several angles of incidence for typical two and three layer models and is shown in graphs.



## INTRODUCTION

To classify the ocean bottom as a reflector, it is of importance to describe the reflectivity in a simple but general way.

One of the most used quantities in this respect is the reflection loss, which, for a given layering system, depends on both frequency and angle of incidence. This method gives the most detailed information but requires several lengthy and complicated calculations.

The use of the distortion of explosive-generated, broad-band pulses gives a very simple, direct picture of the reflectivity but is specific with respect to the used source.

This limitation can be overcome by working with a pulse length that is very short compared with the travel times between the layers, so the reflected signal is an approximation to the impulse response caused by a delta pulse.

The impulse response for a certain angle can be obtained by a Fourier inversion of the frequency-dependent complex reflection coefficient for the same angle. In principle, this operation does not give greater difficulties but a certain care has to be shown at some of the points in the numerical calculations.



## 1. IMPULSE RESPONSE

### 1.1 Theory

Assuming that the bottom can be approximated by a linear and time invariant system, the reflection coefficient  $H(\omega)$  will then represent the transfer function for the system. This means that an input  $f(t)$  with a Fourier transform  $F(\omega) = \int_{-\infty}^{\infty} f(t) e^{-i\omega t} dt$  will result in an output  $g(t)$ , determined by

$$g(t) = \frac{1}{2\pi} \int_{-\infty}^{\infty} F(\omega) \cdot H(\omega) e^{i\omega t} d\omega \quad (\text{Eq. 1})$$

For the delta pulse, also called the Dirac pulse, there exists the pair  $\delta(t) \leftrightarrow 1$  (see e.g. Ref. 1). This, together with Eq. 1, determines the impulse response  $h(t)$  as:

$$h(t) = \frac{1}{2\pi} \int_{-\infty}^{\infty} H(\omega) e^{i\omega t} d\omega \quad (\text{Eq. 2})$$

For a single half-space as a reflector, the transfer function can generally be written in the following way:

$$H(\omega) = \begin{cases} A_0 \cdot e^{i\theta_0} & \omega > 0 \\ A_0 \cdot e^{-i\theta_0} & \omega < 0 \end{cases}$$

or, using the signum function  $\text{sgn } \omega$ ,

$$H(\omega) = A_0 \cdot e^{i\theta_0 \text{sgn}\omega} = A_0 (\cos \theta_0 + i \sin \theta_0 \text{sgn}\omega),$$

which, inserted in Eq. 2, gives

$$h(t) = A_0 \left[ \cos \theta_0 \cdot \frac{1}{2\pi} \int_{-\infty}^{\infty} e^{i\omega t} d\omega + \sin \theta_0 \cdot \frac{1}{2\pi} \int_{-\infty}^{\infty} i \text{sgn}\omega e^{i\omega t} d\omega \right].$$

From the pairs  $\delta(t) \leftrightarrow 1$  and  $\frac{1}{\pi t} \leftrightarrow -i \text{sgn } \omega$  we obtain

$$h(t) = A_0 \cdot \cos \theta_0 \cdot \delta(t) - A_0 \frac{\sin \theta_0}{\pi t} \quad (\text{Eq. 3})$$

which is shown in Fig. 1.



If there is no damping in the present case,  $\theta_0$  will be zero for angles of incidence less than the critical angle ; hence the impulse response is represented by the delta pulse at zero time. Only after the critical angle will there exist a phase shift causing the hyperbolic term in the impulse response.

## 1.2. Numerical Calculations

In the case of a layered bottom,  $H(\omega)$  is generally so complicated that the integral in Eq. 2 has to be calculated by numerical methods. Because of the factor  $e^{i\omega t}$  the integrand will oscillate, thereby making it impossible to use normal quadrature.

By approximating  $H(\omega)$  with a series of straight lines corresponding to a constant-frequency interval length and differentiating twice, we obtain a sequence of equally-spaced delta pulses. These pulses can then be transformed into the time domain and, after some additional calculations, yield the required impulse response. The method is described in detail in Ref. 2.

Later on in the numerical calculations it is necessary to truncate the integral at a frequency high enough for the remainder to be ignored. But there will then exist a finite reflection loss for  $\omega \rightarrow \infty$ , so that any termination of the integral will cause a serious truncation error. To avoid this difficulty we remove from the transfer function the asymptotic value that corresponds to the

case where the upper layer is acting as a half-space reflector:

$$H(\omega) = H(\infty) + T(\omega) ,$$

where

$$T(\omega) \rightarrow 0 \text{ for } \omega \rightarrow \infty .$$

Using Eqs. 2 and 3, the impulse response can be written as

$$h(t) = \text{Re} [H(\infty)] \delta(t) - \frac{\text{Im}[H(\infty)]}{\pi t} + \frac{1}{\pi} \int_0^{\omega_0} T(\omega) e^{i\omega t} d\omega, \quad (\text{Eq. 4})$$

where  $\text{Re} [ \ ]$  and  $\text{Im} [ \ ]$  are respectively the real and imaginary part. The last integral can now be calculated by truncating at  $\omega_0$ , such that  $T(\omega_0) \ll 1$ .

In the case where no damping is present this procedure will not be possible, because  $T(\omega)$  will keep oscillating even for  $\omega \rightarrow \infty$ . Therefore another method has to be used, which we will illustrate by a two-layer model and waves with vertical incidence. If the amplitude of the incident wave is unity, the amplitude of the reflected wave will represent the reflection coefficient. The reflected wave will be composed of the following parts:

- a. Waves reflected from the 1st interface.

b. Waves penetrating the 1st interface, passing through the layer, being reflected from the 2nd interface, and finally passing through the 1st interface again.

c. Waves penetrating the 1st interface, undergoing two reflections from the 2nd interface and one from the 1st before leaving the layer through the 1st interface, etc.

Denoting reflection coefficients by  $H$ , and transmission coefficients by  $P$ , and letting the indices correspond to the layer number as indicated in Fig. 2, we obtain:

$$\begin{aligned}
 H_{\text{ref}} = & H_{10} + \\
 & P_{01} \cdot H_{21} \cdot P_{10} \cdot e^{-2ik_1 d_1} + \\
 & P_{01} \cdot H_{21} \cdot H_{01} \cdot H_{21} \cdot P_{10} \cdot e^{-4ik_1 d_1} , \quad (\text{Eq. 5})
 \end{aligned}$$

where  $2k_1 d_1$  is the phase shift in the layer. Introducing the sound velocity  $\alpha$  and frequency  $\omega$ , this can also be written as  $(2d_1/\alpha_1)\omega$ . The Fourier inversion of Eq. 5 can be carried out by using the pairs  $\delta(t) \leftrightarrow 1$  and  $f(t-t_0) \leftrightarrow F(\omega) e^{-it_0\omega}$ , when  $f(t) \leftrightarrow F(\omega)$ , yielding the impulse response as:

$$\left. \begin{aligned}
 h(t) = & H_{10} \cdot \delta(t) + \\
 & P_{01} \cdot H_{21} \cdot P_{10} \cdot \delta\left(t - \frac{2d_1}{\alpha_1}\right) + \\
 & P_{01} \cdot H_{21} \cdot H_{01} \cdot H_{21} \cdot P_{10} \cdot \delta\left(t - \frac{4d_1}{\alpha_1}\right) + \\
 & \vdots
 \end{aligned} \right\} \quad (\text{Eq. 6})$$

The transmission coefficient will always be positive and, for an increasing impedance through the layers, only the reflection coefficient  $H_{01}$  will be negative. We therefore obtain the impulse response as a sequence of delta pulses separated from each other by the travel time  $(2d_1/\alpha_1)$  and with alternate signs after the 2nd pulse.

At this point it is possible to get an idea of the influence of damping on a separate pulse. Let us consider the first reflection from the second interface and represent the damping by a complex wave number  $k' = k(1 - i\epsilon)$ , which, used with Eq. 5, gives the phase shift:

$$e^{-2ik'd} = e^{-2ikd} \cdot e^{-2k\epsilon d} = e^{-i(2d/\alpha)\omega} \cdot e^{-(2d\epsilon/\alpha)|\omega|}$$

The Fourier inversion is then carried out by the use of the pairs  $e^{-\beta|t|} \leftrightarrow 2\beta/(\beta^2 + \omega^2)$  and  $F(t) \leftrightarrow 2\pi f(-\omega)$ , when  $f(t) \leftrightarrow F(\omega)$ , resulting in the second pulse given by

$$P_{01} \cdot H_{21} \cdot P_{10} \frac{d_1 \epsilon_1 / \alpha_1}{\pi \left( 4(d_1 \epsilon_1 / \alpha_1)^2 + (t - 2d_1 / \alpha_1)^2 \right)}$$

In this case it is not a delta pulse, but a "gaussian-looking" pulse that is obtained; thus increased damping will decrease the peak amplitude but widen the pulse.

Working with plane waves, a physical requirement is a causal response for vertical incidence because, except for vertical incidence, one can consider the reflection as starting at time 'minus infinity'. Assuming at this point that  $\text{Im}[H(\infty)] = 0$ , this means that the last term has to be causal. To obtain this it is very important in the calculations to use the right asymptotic value of  $H(\omega)$  calculated from the top layer as half-spaced. Figure 3 shows the result for vertical incidence and near-zero time, when using the value of  $H$  as bias at  $\omega_0$  and at infinity. The parameters for the model used are given in Fig. 2.

For the same model and incidence, the effects of the truncating frequency and frequency increments on the shape of the second pulse are shown in Figs. 4 and 5. The error caused by a too early truncation shows very clearly in Fig. 4.

Returning to the requirement of causality, this is not fulfilled by the second term in Eq. 4 except when  $\text{Im}[\ ] = 0$ . Under the same assumption of a finite and constant damping  $\delta$  pr. wave length, the damping will be unlimited for  $\omega \rightarrow \infty$ . Therefore, for  $\omega \rightarrow \infty$ ,  $\delta$  must trend towards zero, which in means that the phase shift, and thereby the imaginary part of the loss, must also approach zero. Since we are not able to describe the exact way that the damping behaves for infinite frequencies we will maintain the chosen model, but will remember the cause for the non-causality in case of vertical incidence.

Had the damping in the water been taken into account, the reflection from the first interface would not have been a perfect delta pulse but a finite pulse, as the reflection from the second interface.

Because of the asymmetry around  $t = 0$  for the hyperbolic term, the effect when using the impulse response for convolution will be negligible for signals of a certain length, which again agrees with the limited frequency band for such a signal.

## 2. NUMERICAL EXAMPLE

To illustrate the method, the impulse response for a two-layer and a three-layer model has been calculated and plotted for the following angles of incidence:  $0^\circ$ ,  $40^\circ$ ,  $60^\circ$ ,  $80^\circ$ . The data for the two models are given in Fig. 2. On the results shown in Figs. 6-13 the delta pulses are indicated by solid arrows with a length proportional to their value and sign.

Looking, for example, at Fig. 11, which shows the impulse response for the three-layer model and  $40^\circ$  incidence, we notice the following reflections: first the delta pulse and the hyperbolic term from the surface, then the gaussian-looking pulse from the second interface. Because the critical angle for the half-space is  $32.3^\circ$ , the reflection from the third interface will involve a phase shift, which gives the pulse from this layer an inverted look. The next pulse to be seen on the figure occurs at  $t \approx 4.5$  and is caused by the reflection of the previous pulse from the first and second interfaces before leaving this layer through the first interface. The pulse will have the same polarity as the incident because an additional reflection from the first interface separating a higher from a lower impedance. The following pulses are difficult to trace exactly because of the repeated influence of the phase shift. The closing-in of the pulses with increasing angle of incidence is



caused by the geometrical phase shift in the layer. For vertical incidence, Eq. 5 gives the phase shift as  $(2d/\alpha)\omega$ , which, for other angles of incidence, has to be multiplied by  $\cos \theta$ , where  $\theta$  is the angle between the layer normal and the ray in the layer. Therefore, in the impulse response, the pulses will be spaced by  $(2d/\alpha) \cos \theta$  when the angle of incidence is less than the critical angle associated with the critical reflection.

A direct comparison with experimental data is rather difficult because of the need for a short time constant, which, in practice, limits the peak amplitude and thereby the penetration depth. A compromise must therefore be made, and we have considered the reflection, at three different angles of incidence, of an experimental shock pulse having a time constant at about 0.3 - 0.4 ms (Ref. 3).

The analysis of the reflection losses using octave band filters indicates a critical angle of about  $60^\circ$  and relative densities of 1.4 and 2.3. The reflected pulses suggest that we are dealing with at least an upper layer where the critical angle is larger than  $70^\circ$  and a lower layer where the critical angle is less than  $70^\circ$ . On the basis of this information the 4-layer model shown in Fig. 14 was constructed, and the impulse responses were calculated for angles of incidence of  $70^\circ$ ,  $74.5^\circ$ , and  $81.5^\circ$ , as shown in Figs. 15a, 15b, & 15c. These theoretical response curves are seen to agree well with the corresponding experimental curves plotted on the same figures.



## REFERENCES

1. A. Papoulis, "The Fourier Integral and its Applications," Mc Graw-Hill, 1962.
2. O.F. Hastrup, "Distortion of Bottom Reflected Pulses," SACLANTCEN T.R. No. 51, March 1966, NATO UNCLASSIFIED.
3. B. Lallement, SACLANTCEN. Private communication.



	Compressional velocity	Shear velocity	Damping in dB/wave-length for $\alpha$ and $\beta$ waves	Density	Thickness
(0)	$\alpha = 100$	$\beta = 0$	$a = 0$	$\rho = 1.0$	$d = \infty$
(1)	1.055	0.26	1.0	1.89	1.00
(2)	1.13	0.40	1.5	2.05	1.50/ $\infty$
(3)	1.87	1.07	0.5	2.20	$\infty$

Layers (0), (1), & (2) are used for two-layer model and Layers (0), (1), (2), & (3) for three-layer model.

Fig. 2



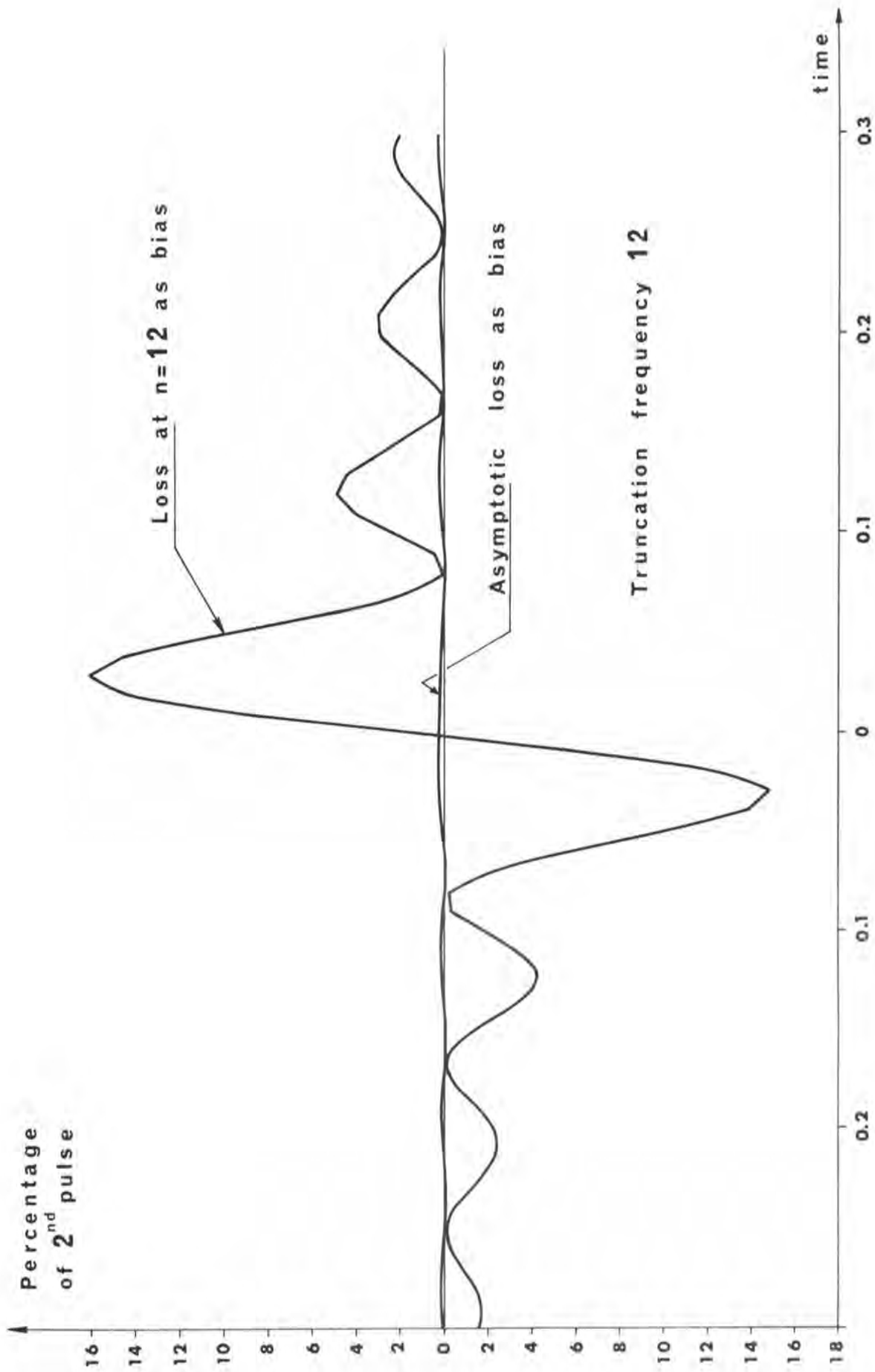


FIG. 3 INFLUENCE OF BIAS ON THE IMPULSE RESPONSE NEAR TIME ZERO



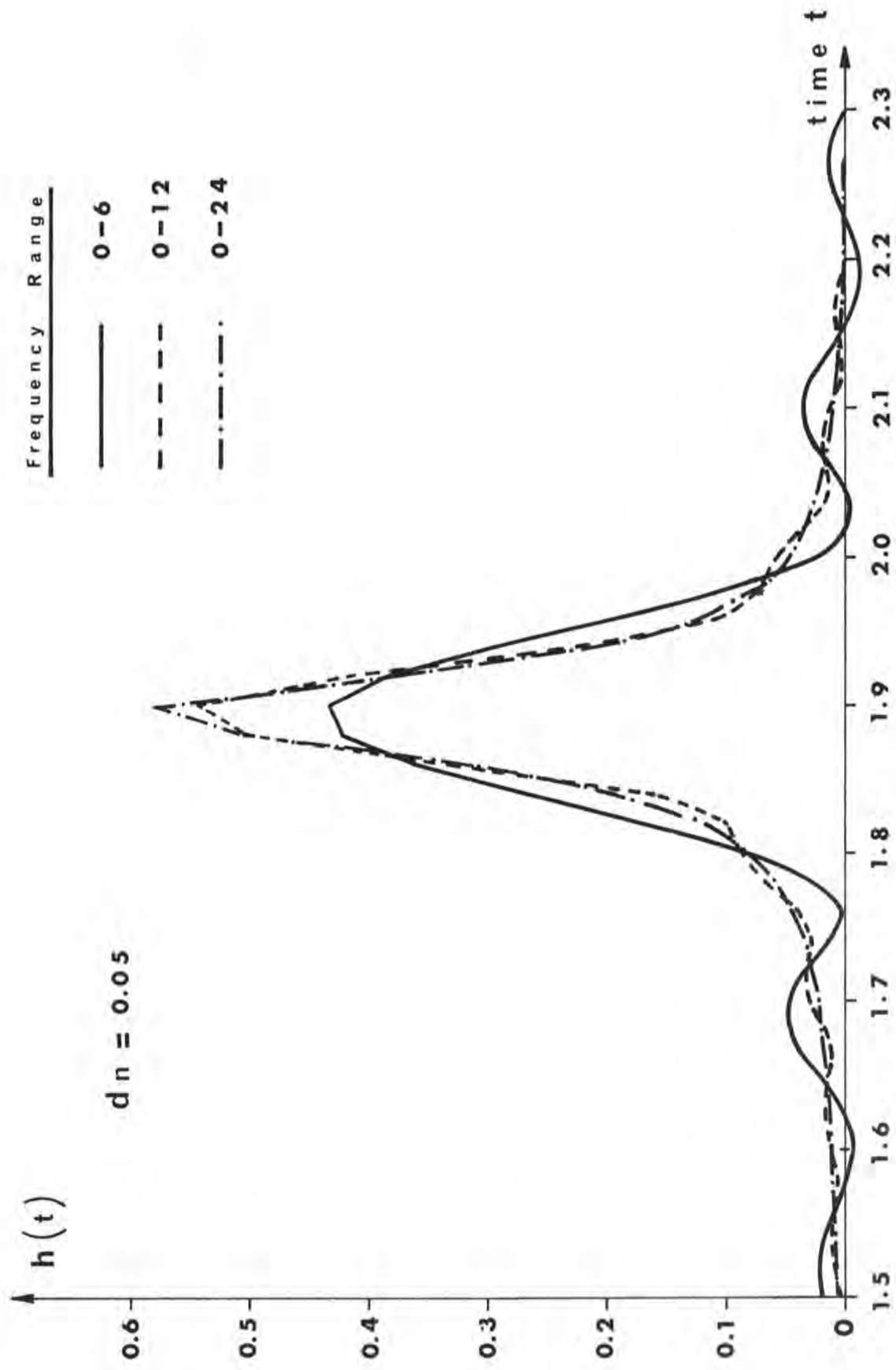


FIG. 4 THE EFFECT OF TRUNCATION FREQUENCY ON THE SHAPE OF THE SECOND PULSE





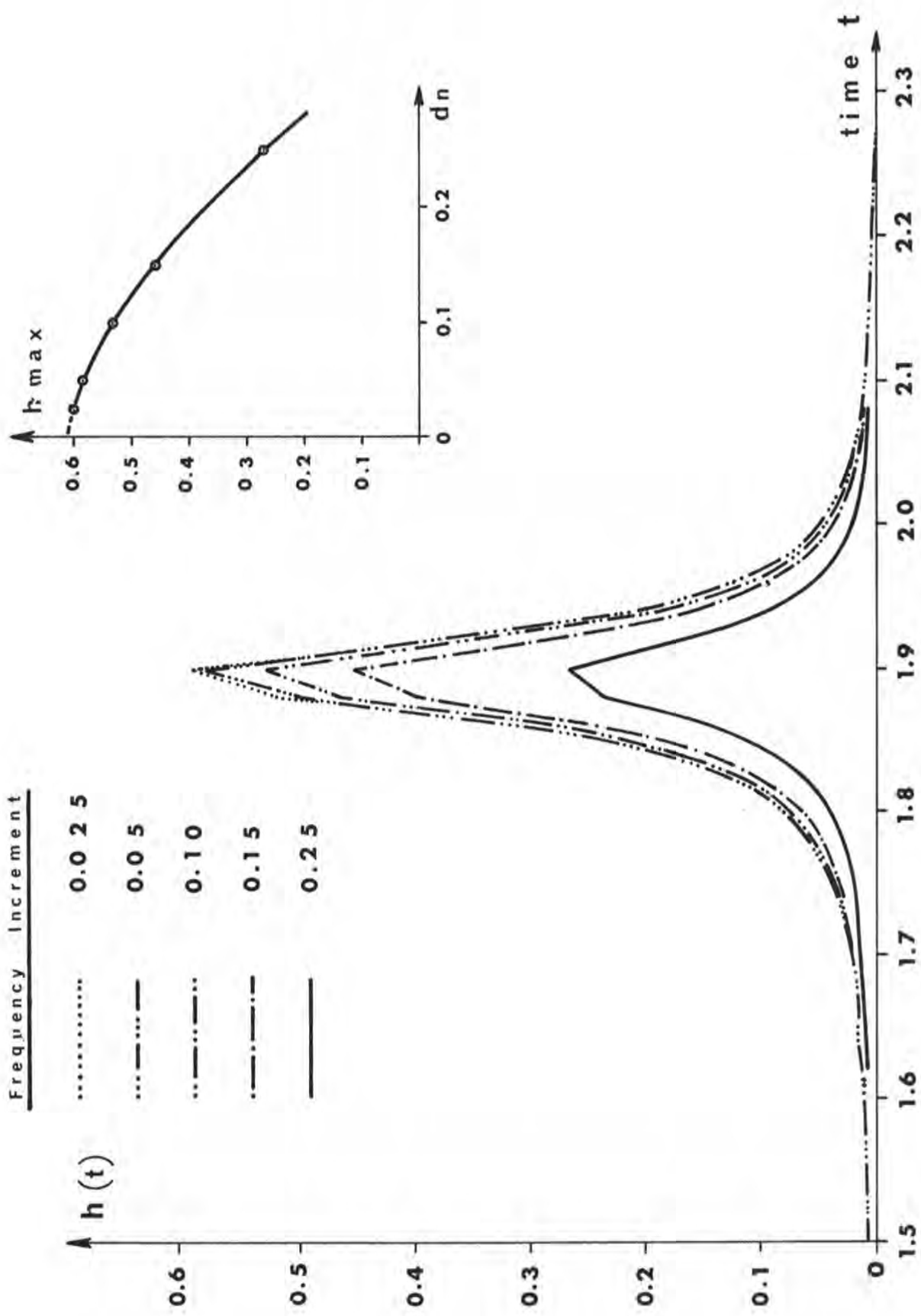


FIG. 5 THE EFFECT OF FREQUENCY INCREMENT ON THE SHAPE OF THE SECOND PULSE



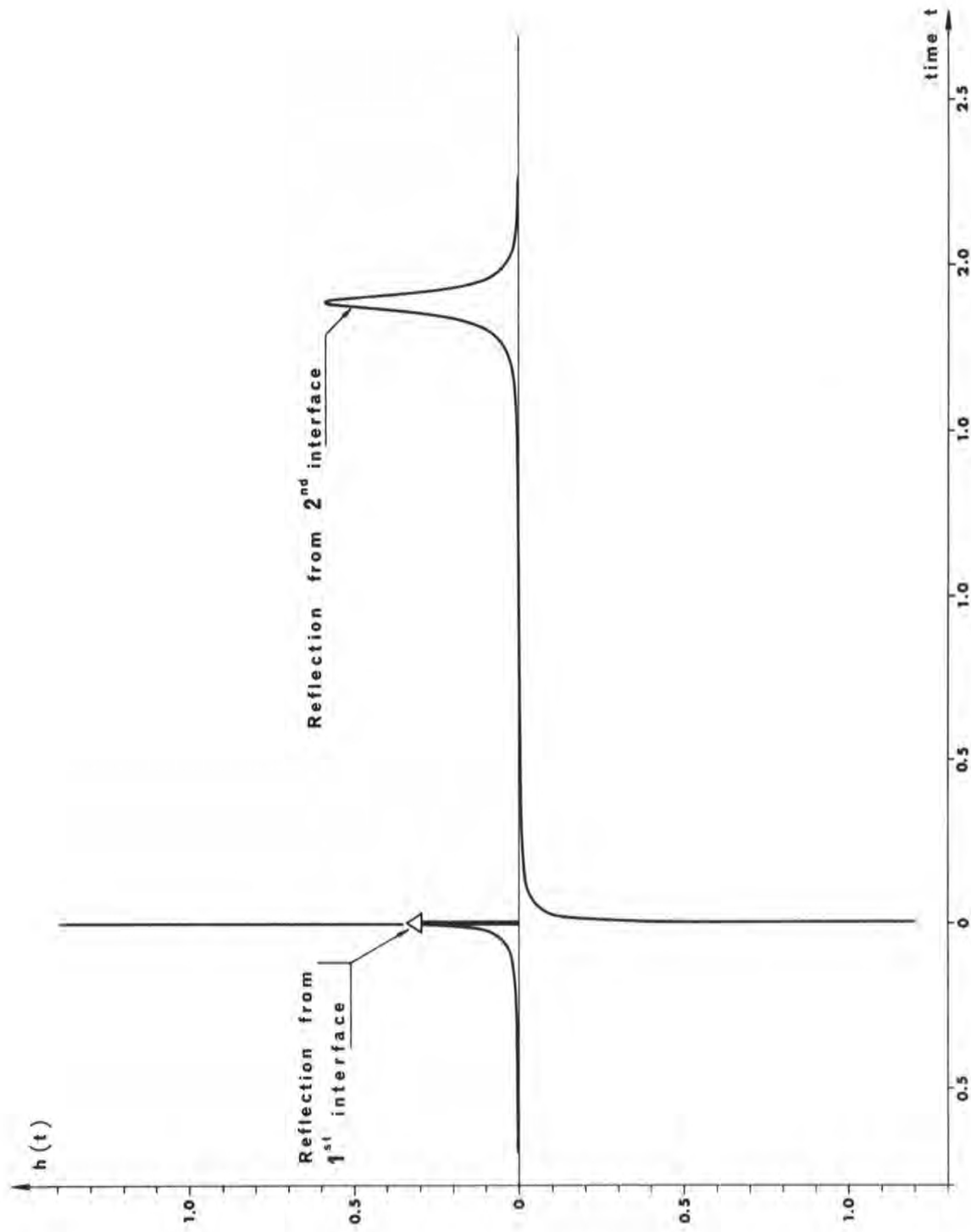


FIG. 6 THE IMPULSE RESPONSE FOR A TWO-LAYER MODEL,  $0^\circ$  INCIDENCE



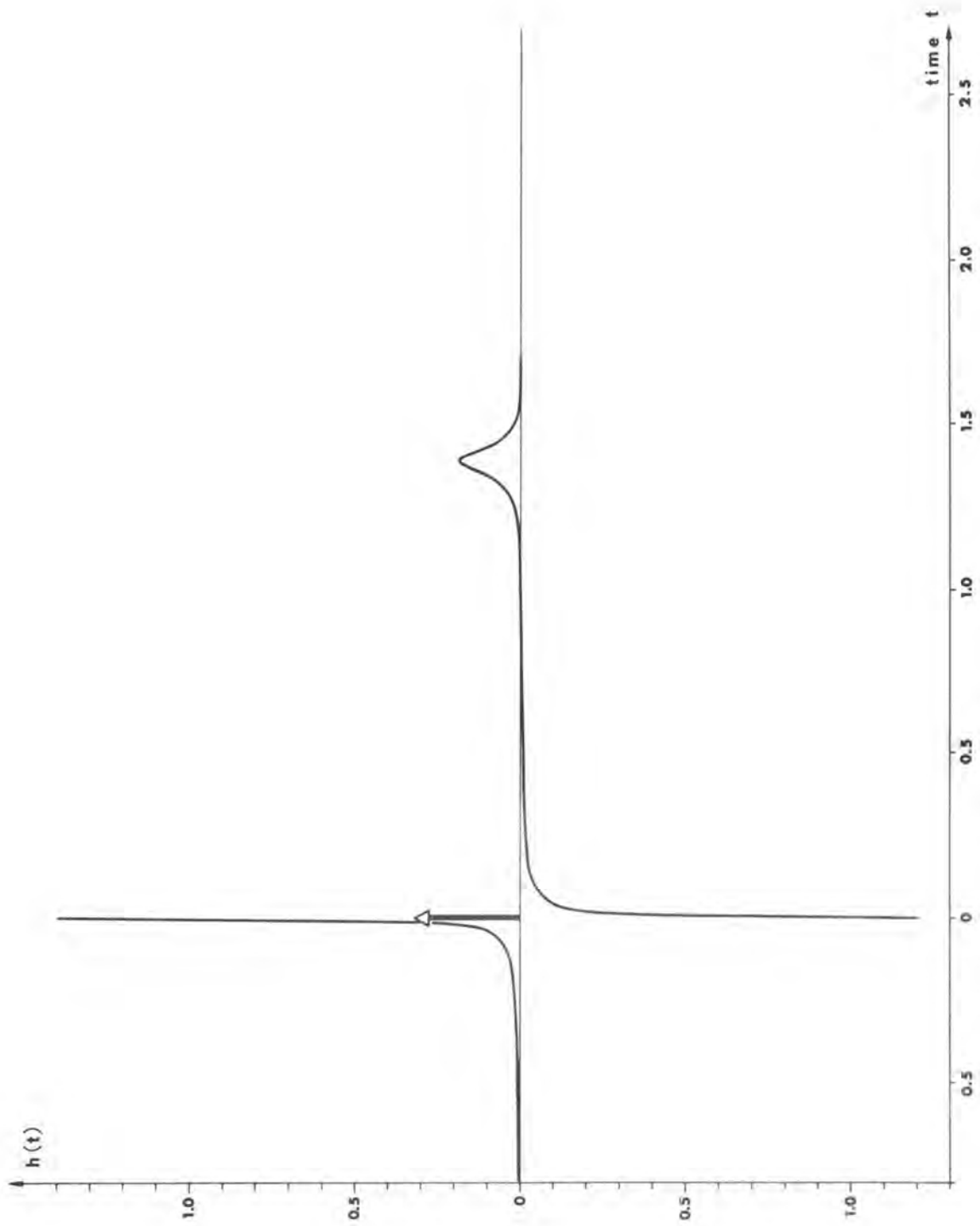


FIG. 7 THE IMPULSE RESPONSE FOR A TWO-LAYER MODEL, 40° INCIDENCE



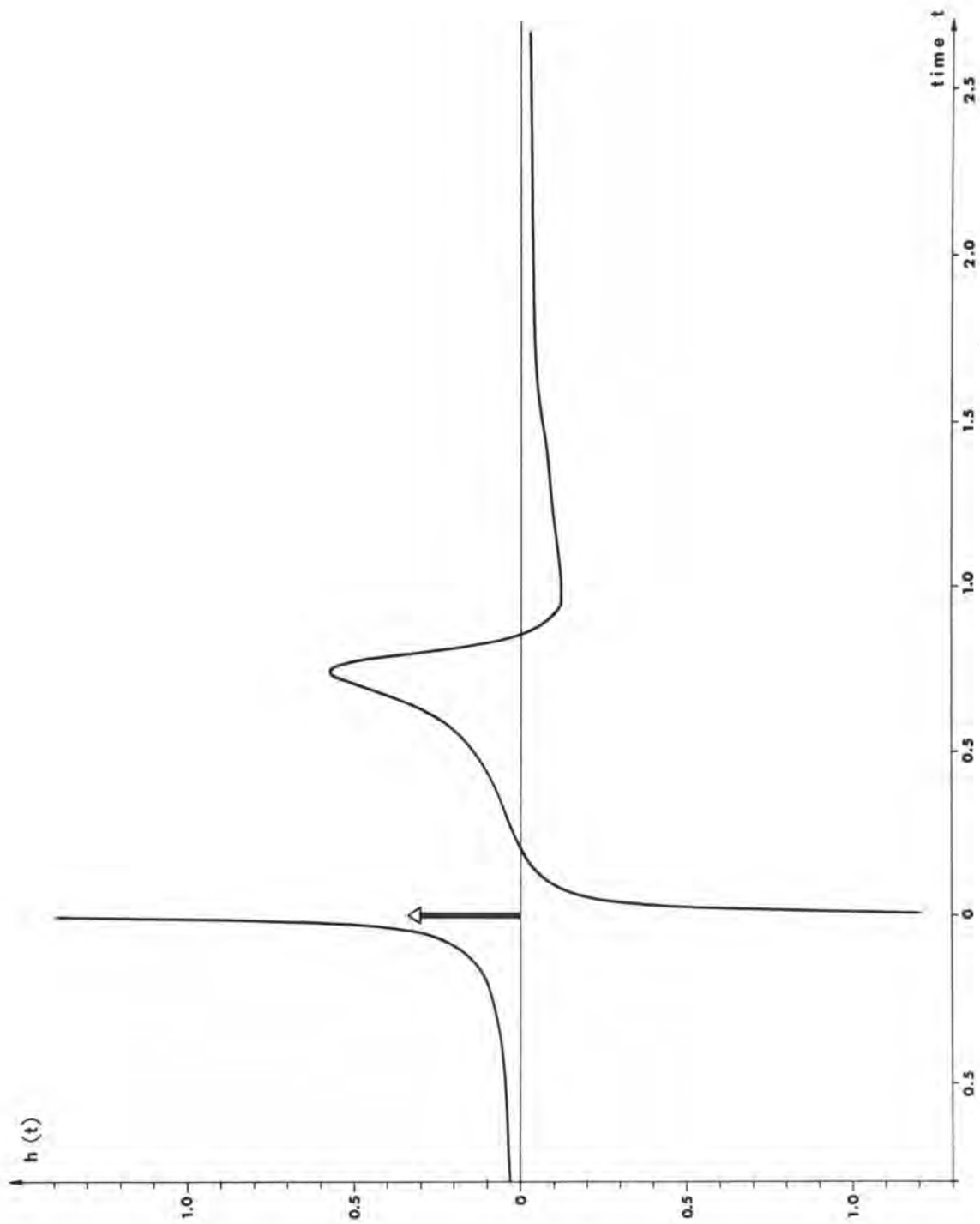


FIG. 8 THE IMPULSE RESPONSE FOR A TWO-LAYER MODEL, 60° INCIDENCE





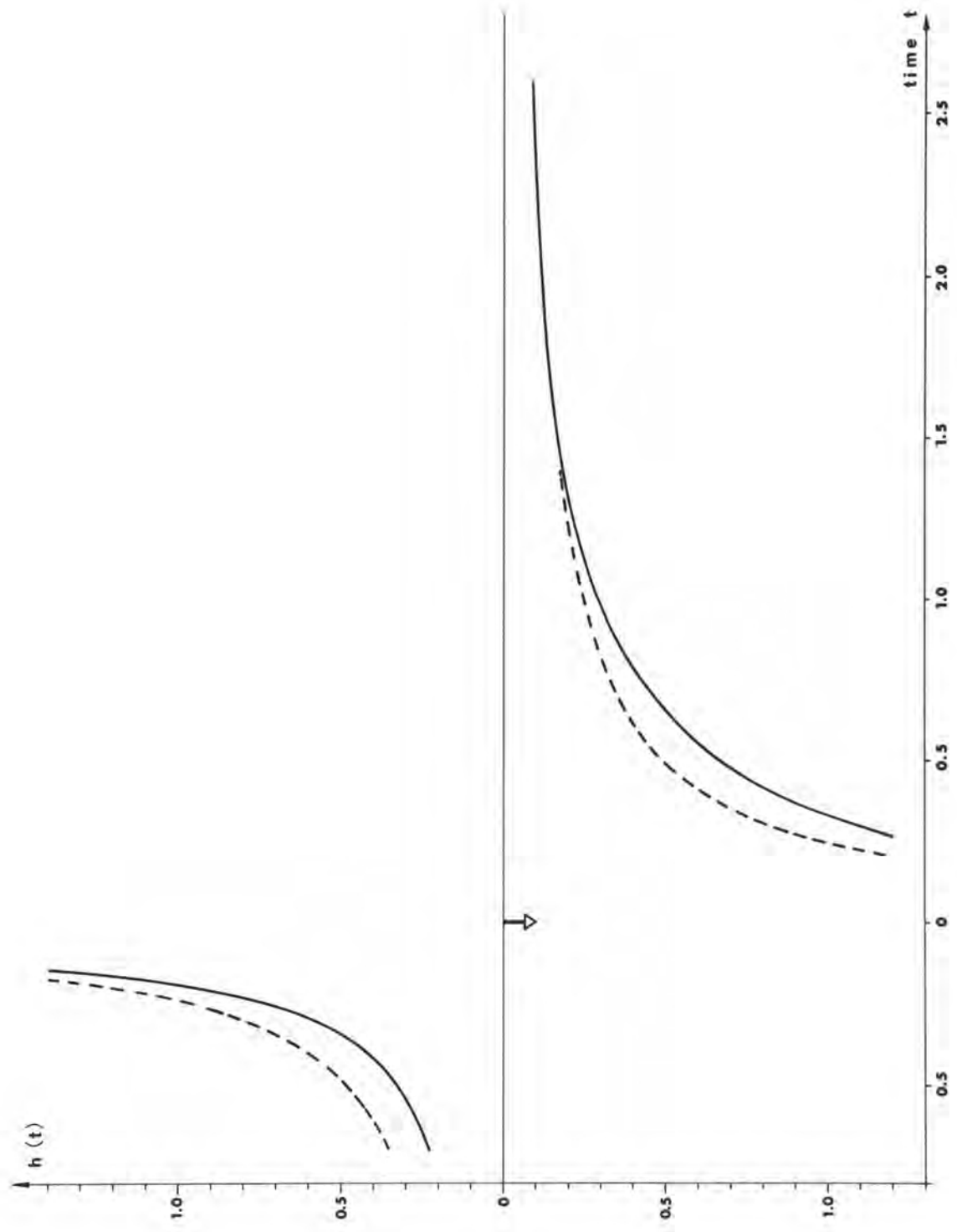


FIG. 9 THE IMPULSE RESPONSE FOR A TWO-LAYER MODEL, 80° INCIDENCE



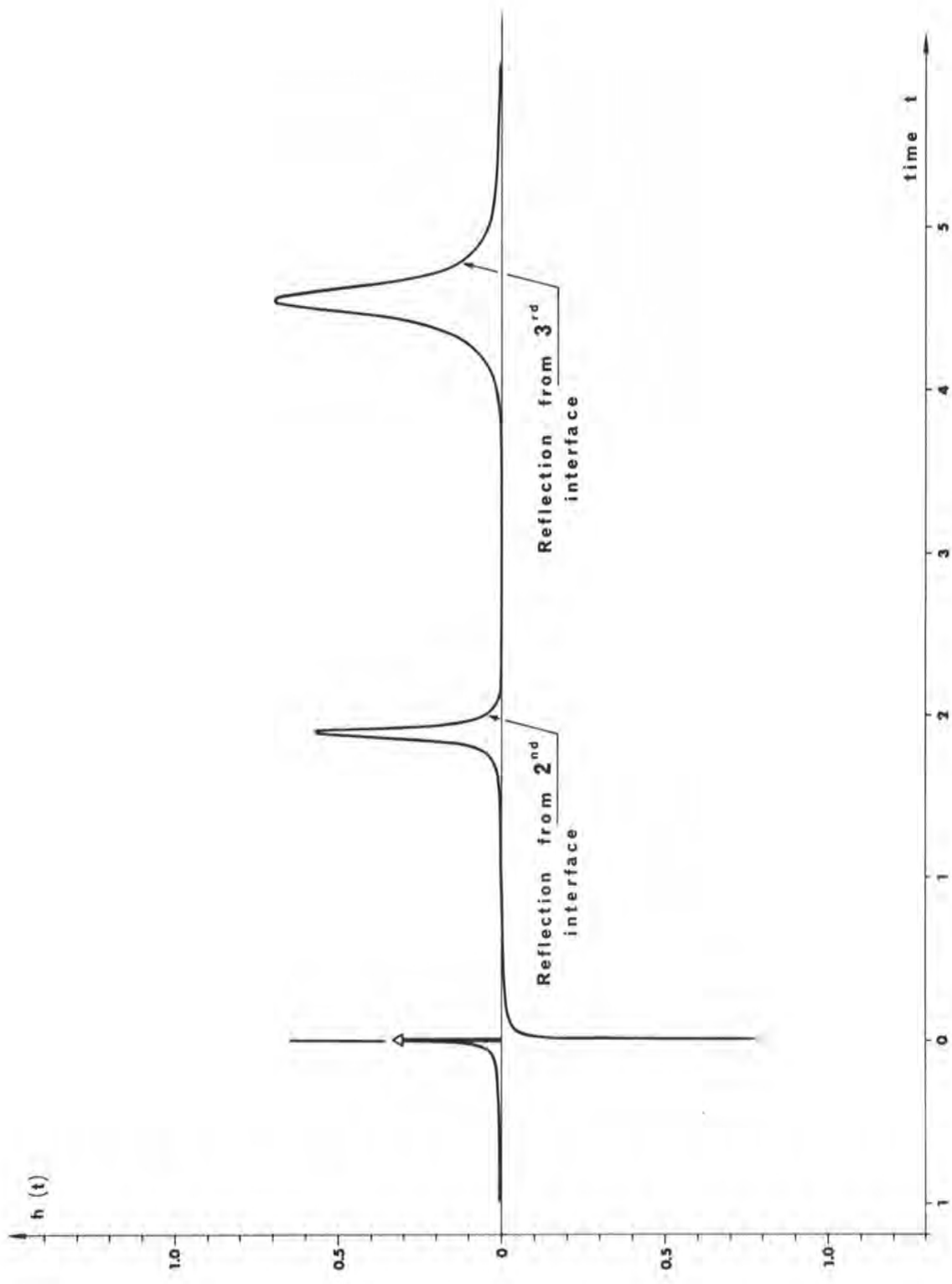


FIG. 10 THE IMPULSE RESPONSE FOR A THREE-LAYER MODEL, 0° INCIDENCE



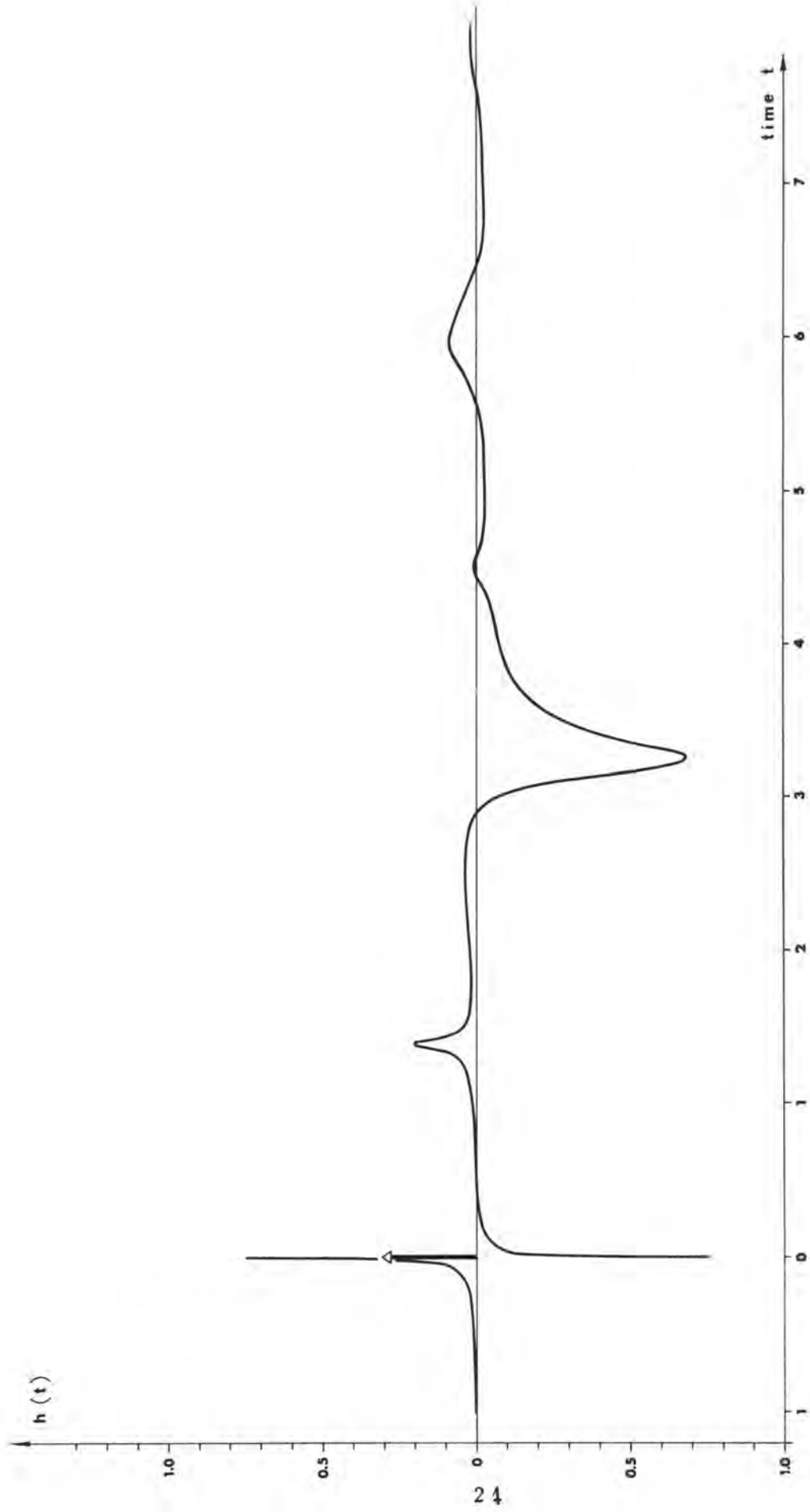


FIG. 11 THE IMPULSE RESPONSE FOR A THREE-LAYER MODEL, 40° INCIDENCE



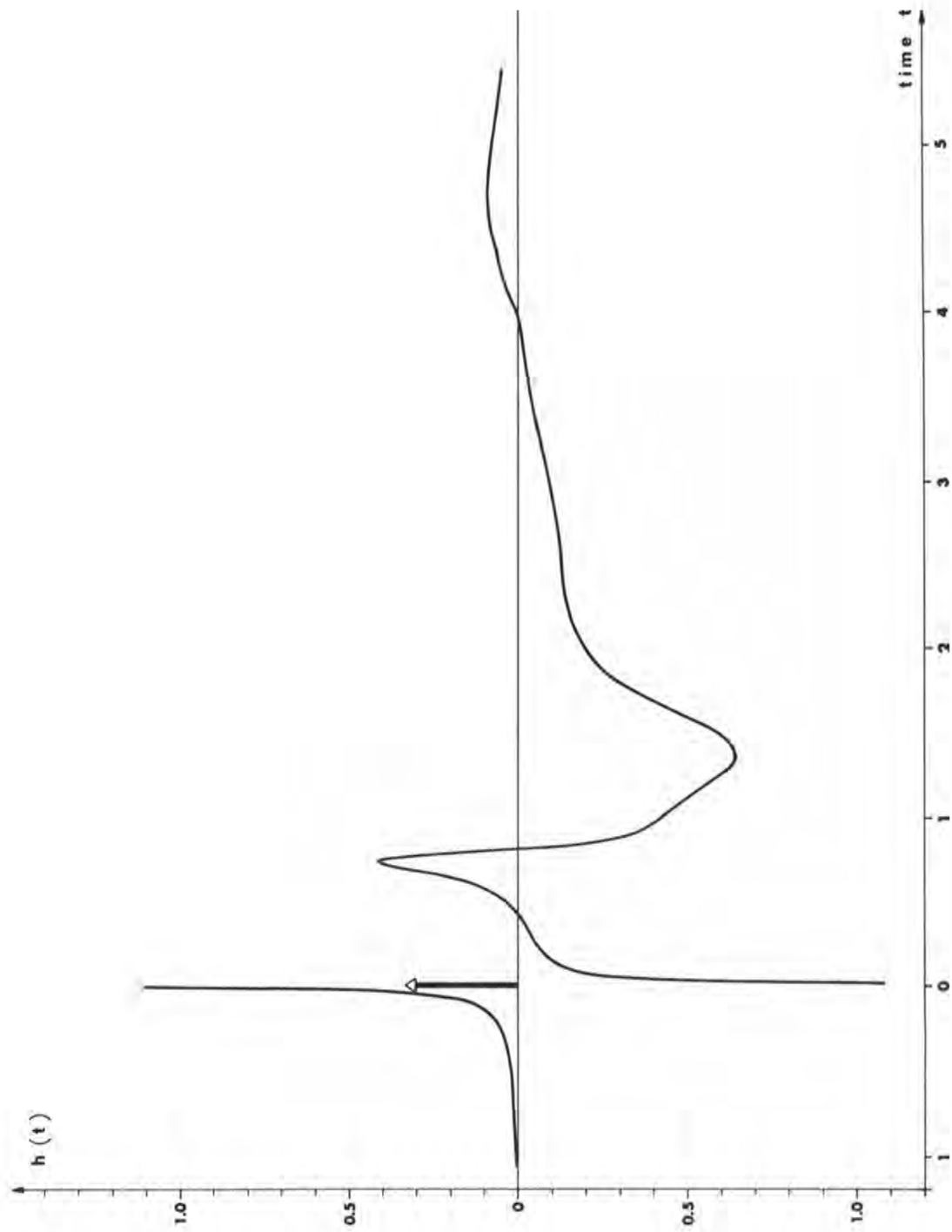


FIG. 12 THE IMPULSE RESPONSE FOR A THREE-LAYER MODEL, 60° INCIDENCE





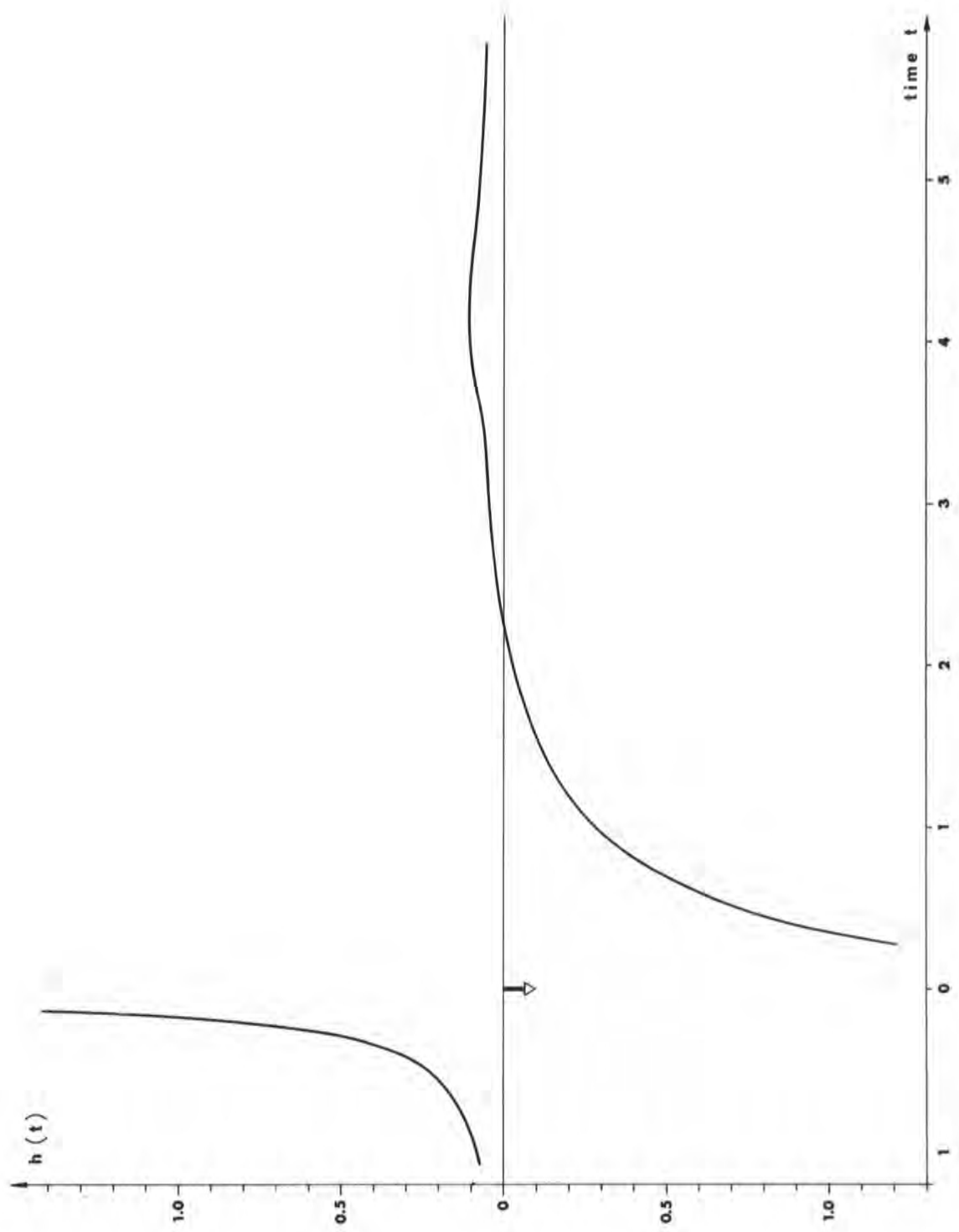


FIG. 13 THE IMPULSE RESPONSE FOR A THREE-LAYER MODEL, 80° INCIDENCE



$\alpha$	$\beta$	dB/wavelength		$\rho$
1.00				1.00
0.97	0.01	1.20	0.01	1.35
1.15	0.40	1.50	2.00	2.20
1.20	0.40	1.50	2.00	2.30
0.98	0.05	1.50	0.05	1.40

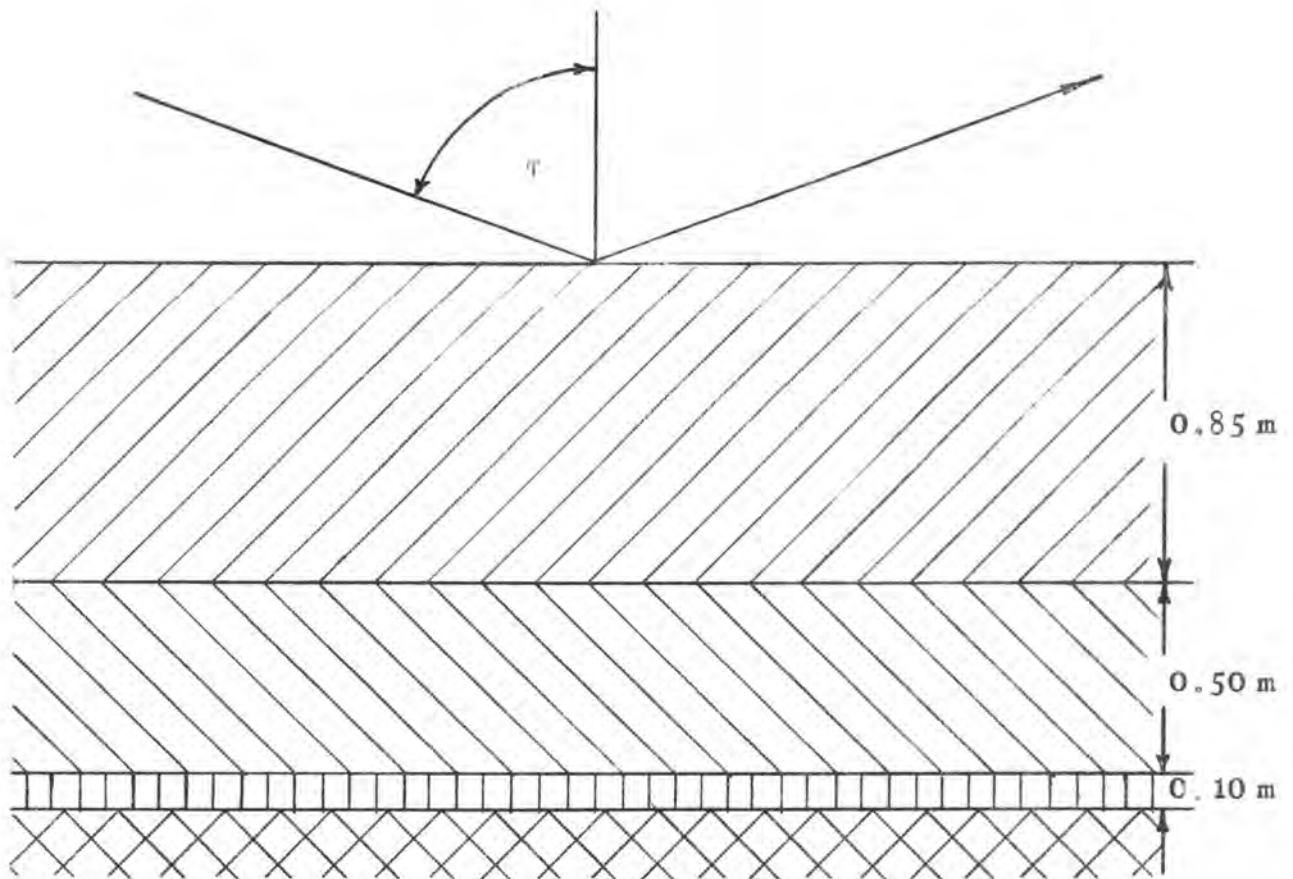
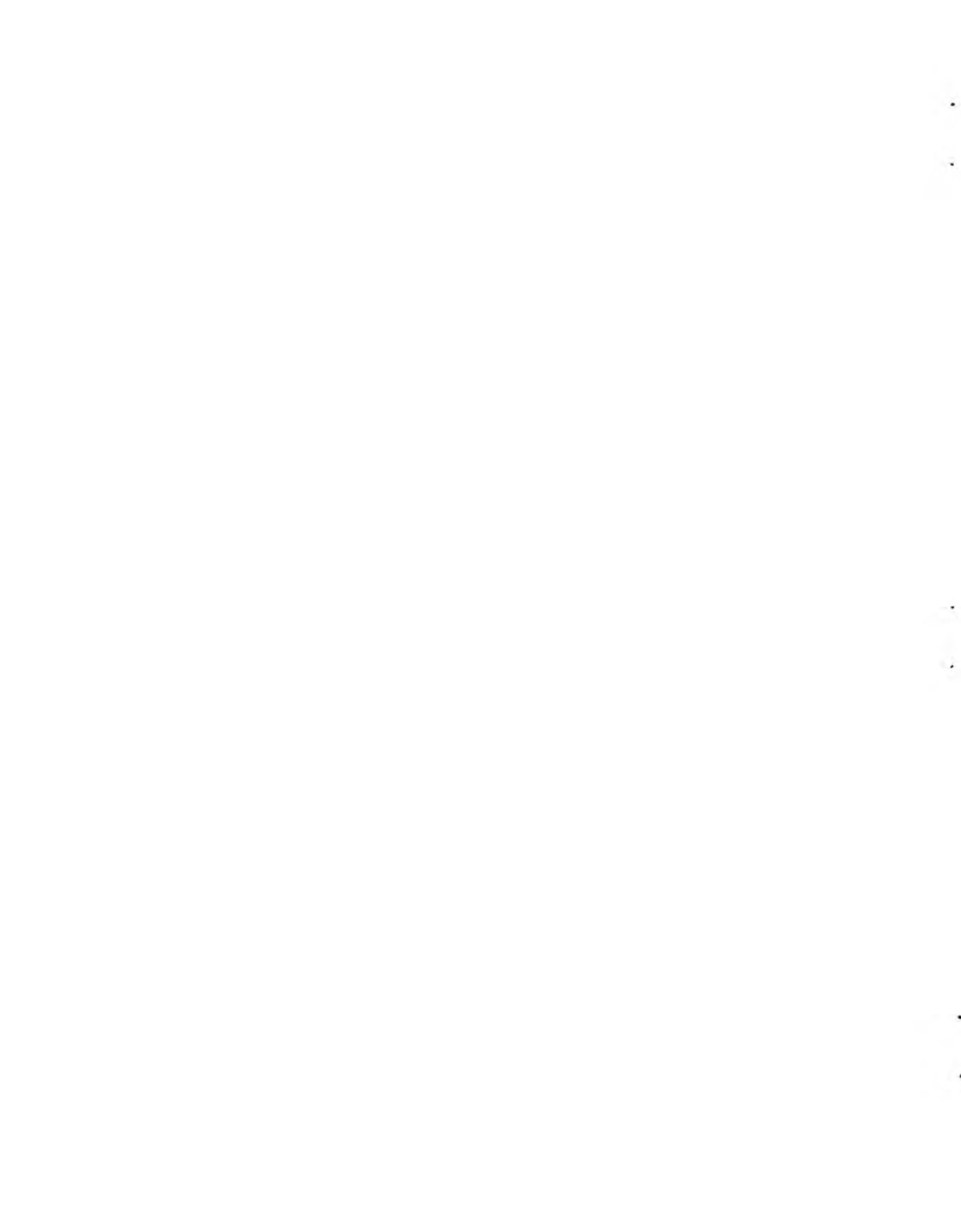


FIG. 14 LAYERING CONSTANTS FOR FIGS. 15a, b & c



Angle of incidence  
 $70^\circ$

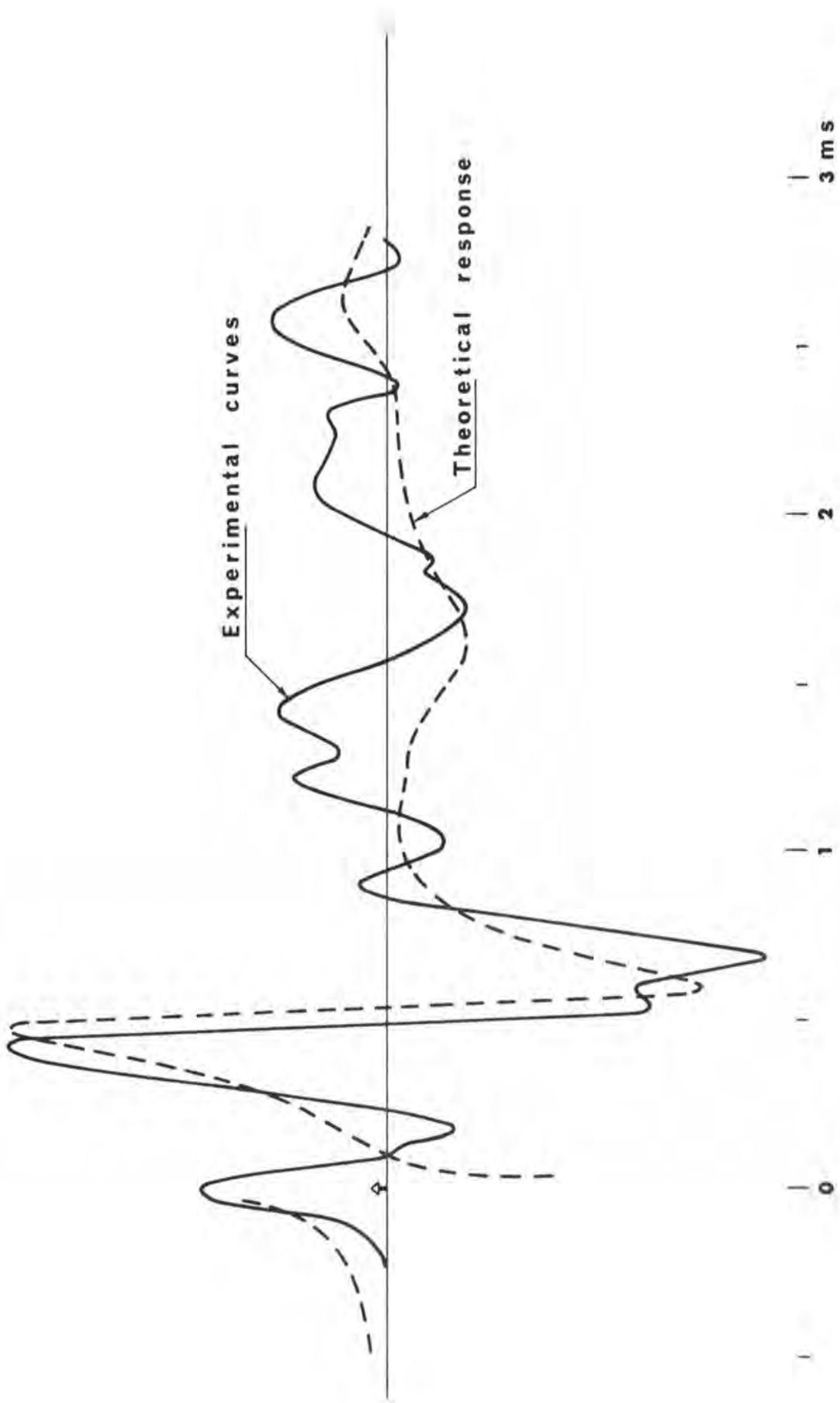


FIG. 15a COMPARISON BETWEEN EXPERIMENTAL AND THEORETICAL PULSE SHAPES



Angle of incidence  
 $74.5^\circ$

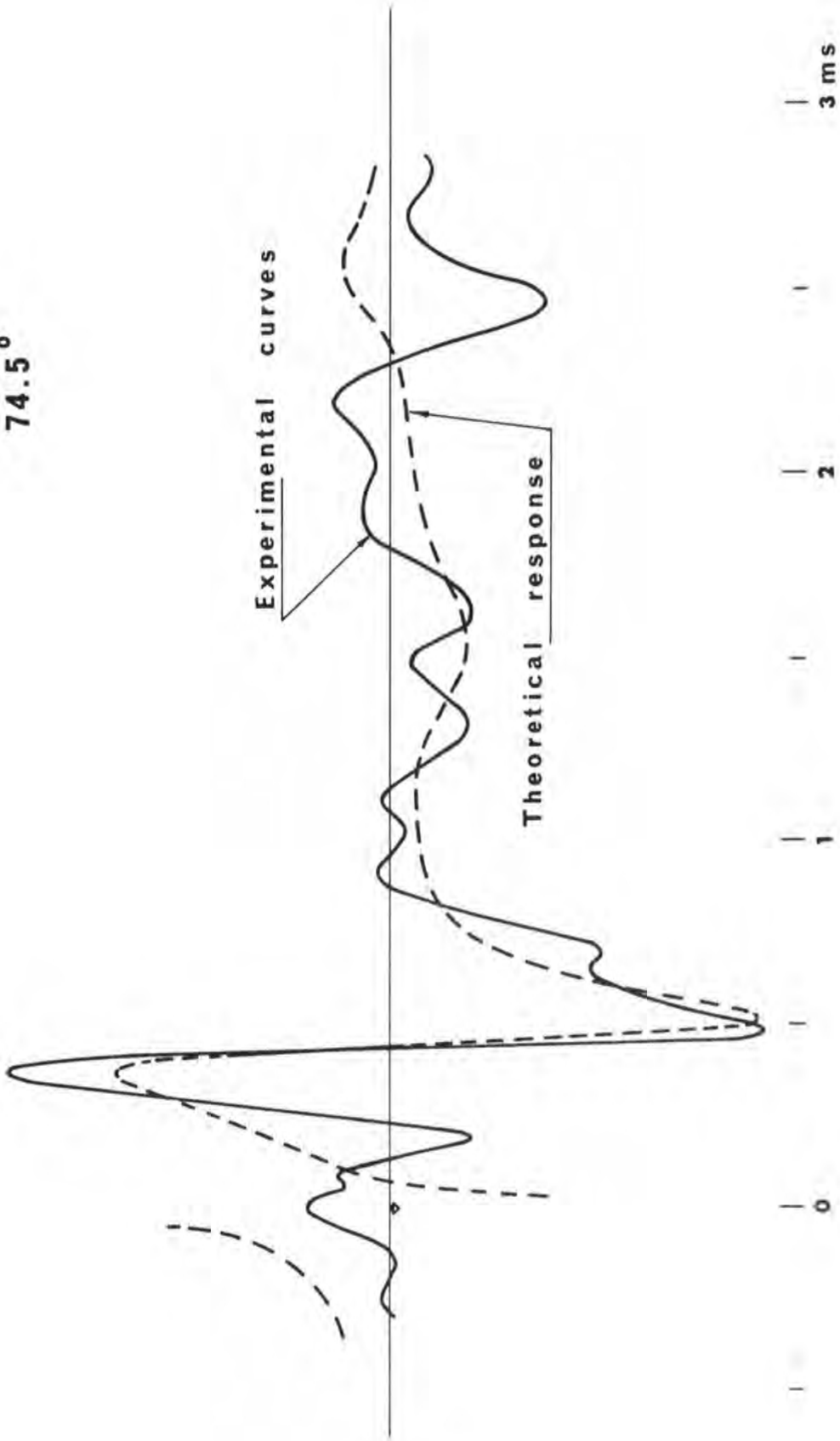


FIG. 15b COMPARISON BETWEEN EXPERIMENTAL AND THEORETICAL PULSE SHAPES





Angle of incidence  
 $81.5^\circ$

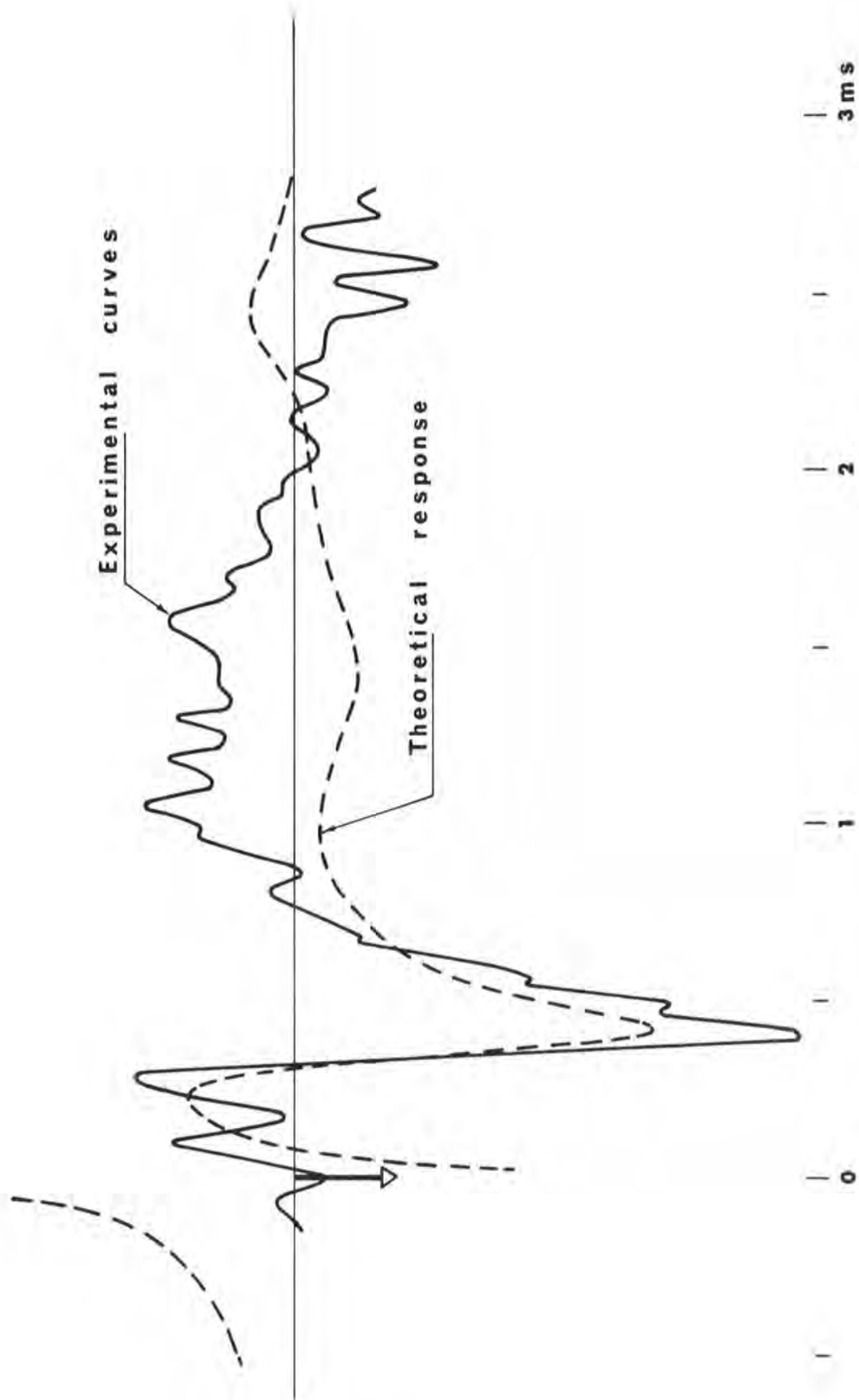
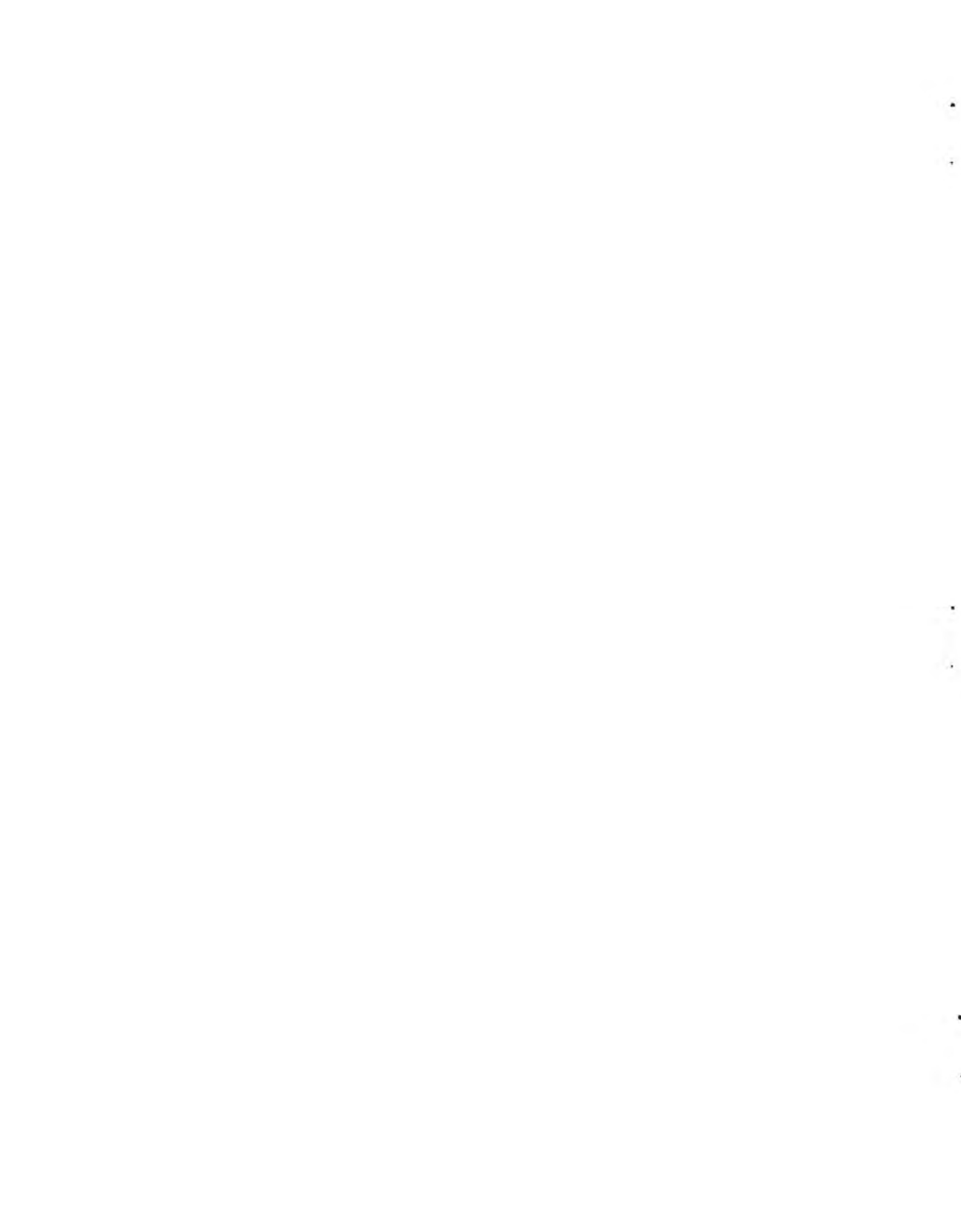
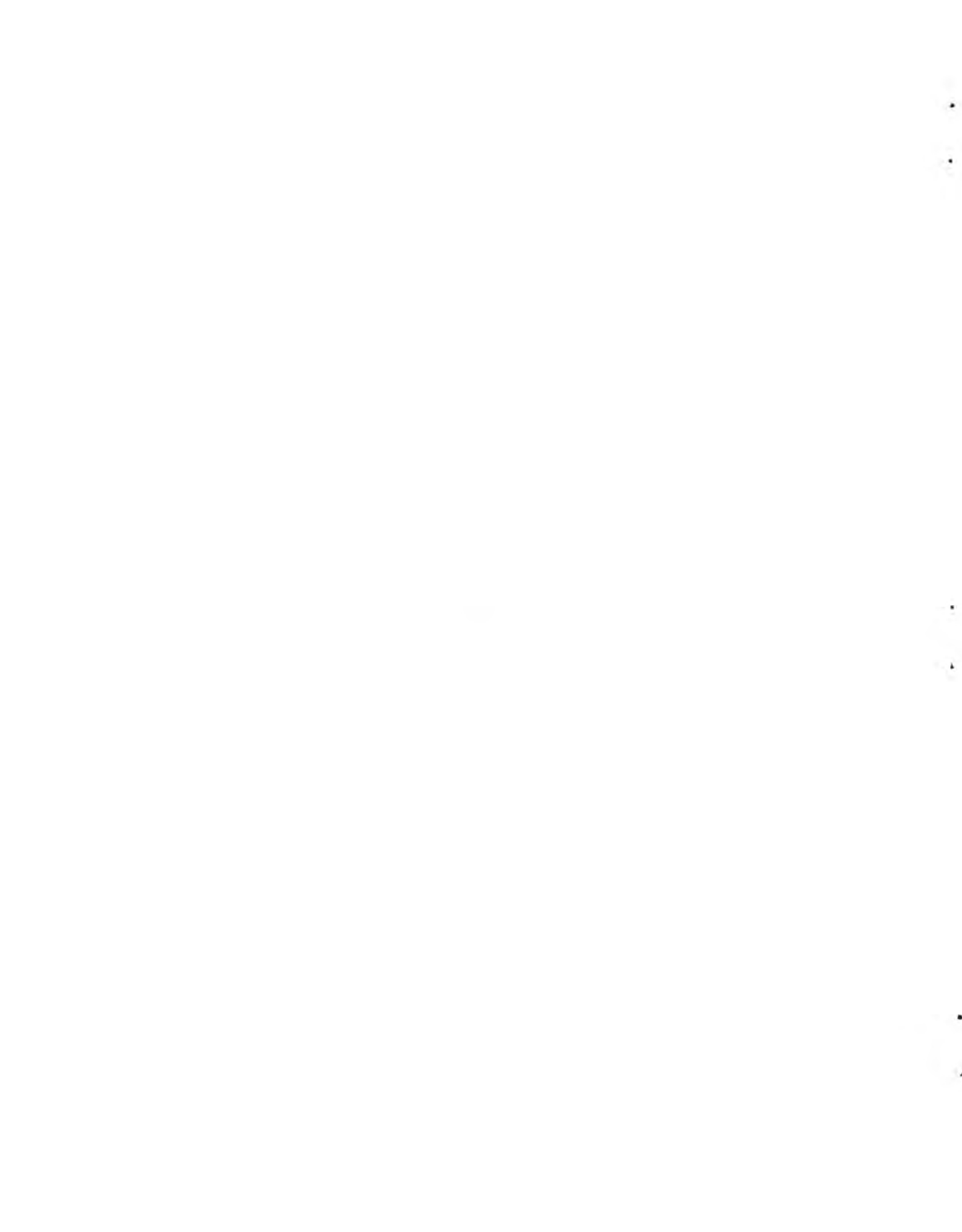


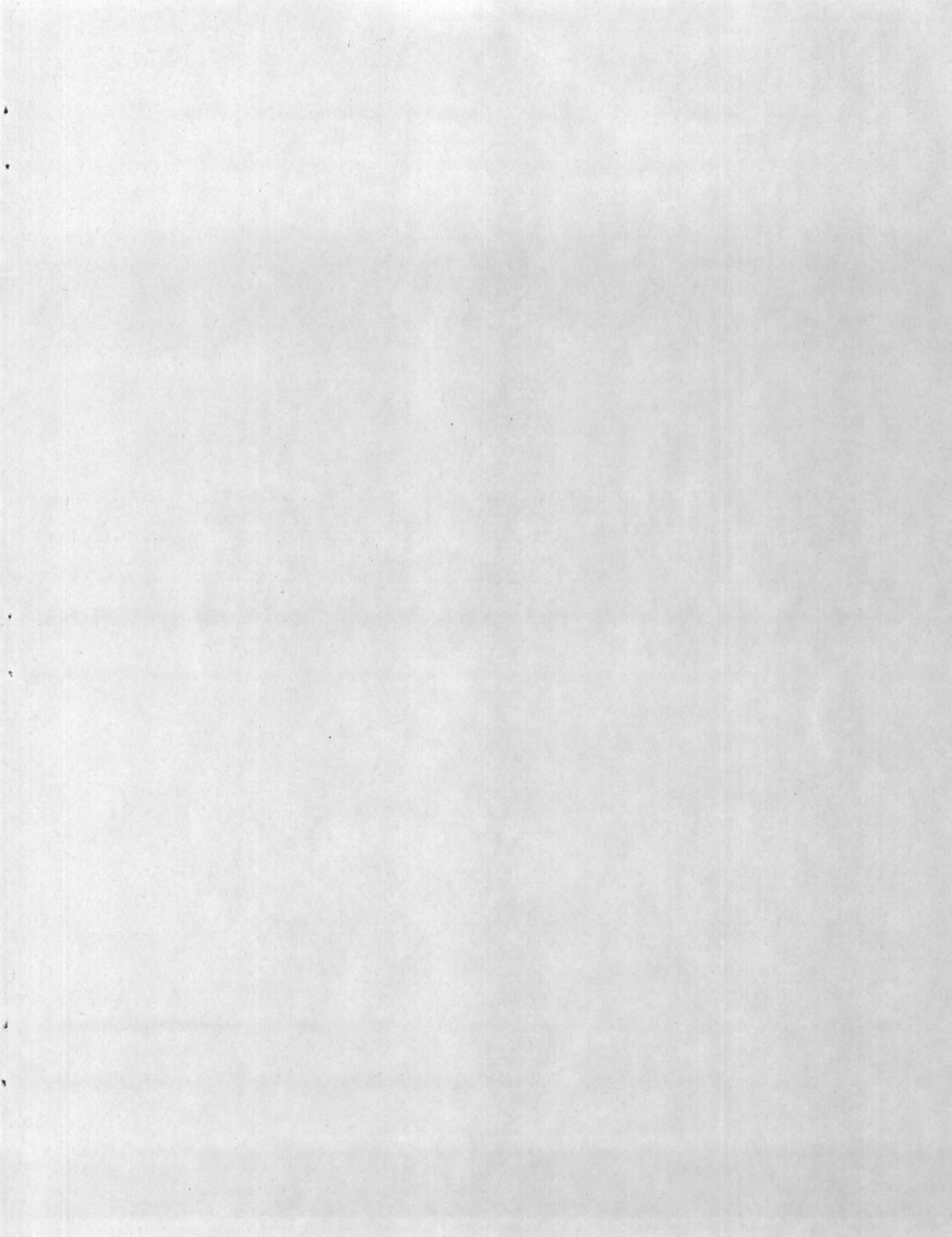
FIG. 15C COMPARISON BETWEEN EXPERIMENTAL AND THEORETICAL PULSE SHAPES



# DISTRIBUTION LIST

	COPIES			COPIES	
	TR	TM		TR	TM
<b>MINISTRIES OF DEFENCE</b>			<b>SCNR for SACLANTCEN</b>		
MOD Belgium	5	5	SCNR Belgium	1	1
MOD Canada	10	10	SCNR Canada	1	1
MOD Denmark	10	10	SCNR Denmark	1	1
MOD France	8	8	SCNR France	1	1
MOD Germany	13	6	SCNR Germany	1	1
MOD Greece	11	11	SCNR Greece	1	1
MOD Italy	8	8	SCNR Italy	1	1
MOD Netherlands	10	10	SCNR Netherlands	1	1
MOD Norway	10	7	SCNR Norway	1	1
MOD Portugal	5	5	SCNR Turkey	1	1
MOD Turkey	3	3	SCNR U.K.	1	1
MOD U.K.	20	20	SCNR U.S.	1	1
SECDEF U.S.	70	70			
<b>NATO AUTHORITIES</b>			<b>NATIONAL LIAISON OFFICERS</b>		
SECGEN NATO	1	1	NLO France	1	1
NATO Military Committee	2	2	NLO Italy	1	1
ASG for Scient. Affairs NATO	1	0	NLO Portugal	1	1
SACLANT	3	1	NLO U.S.	1	1
SACEUR	3	3	<b>NLR to SACLANT</b>		
CINCHAN	1	1	NLR Belgium	1	1
SACLANTREPEUR	1	1	NLR Canada	1	1
CINCAFMED	1	1	NLR Denmark	1	1
CINWESTLANT	1	0	MM France	1	0
COMSUBEASTLANT	1	1	NLR Germany	1	1
COMCANLANT	1	1	NLR Greece	1	1
COMOCEANLANT	1	1	NLR Italy	1	1
COMEDCENT	1	1	NLR Norway	1	1
COMSUBACLANT	1	1	NLR Portugal	1	1
COMSUBMED	1	1	NLR Turkey	1	1
CDR Task Force 442	1	1	NLR U.K.	1	1





**[REDACTED] UNCLASSIFIED**

**[REDACTED] UNCLASSIFIED**